

## Exploring the decay probability of neutron-rich superheavy nuclei

M. Bhuyan\* and B. V. Carlson†

*Instituto Tecnológico de Aeronáutica, 12.228-900 São José dos Campos, São Paulo, Brazil*

(Dated: March 9, 2022)

The modes of decay for the even-even isotopes of superheavy nuclei of  $Z = 118$  and  $120$  with neutron number  $160 \leq N \leq 204$  are investigated in the framework of the axially deformed relativistic mean field model. The asymmetry parameter  $\eta$  and the relative neutron-proton asymmetry of the surface to the center ( $R_\eta$ ) are estimated for the ground state density distributions of the nuclei. We suggest that the resulting asymmetry parameter  $\eta$  and the relative neutron-proton asymmetry  $R_\eta$  of the density play a crucial role in the preformation factor of the decay half life.

PACS numbers: PACS: 21.10.Dr, 21.60.Jz, 23.60.+e, 27.90.+b

Over the last three decades, the synthesis of superheavy nuclei has been dramatically rejuvenated owing to the emergence of cold fusion reactions, performed mainly at GSI, Darmstadt [1–5], and hot fusion and/or the actinide based fusion reactions performed mainly at JINR, Dubna [6–11]. Through these advancements of stable nuclear beam technology, it is not only possible to synthesize superheavy nuclei but also provide impressive prospects for understanding the nuclear properties of these nuclei [1–12]. At present, the question of the mode of decay and the stability of these newly synthesized nuclei arises. While reviewing the production and decay properties of nuclei with atomic number  $100 \leq Z \leq 118$ , it can be seen that the sustainability of these superheavy nuclei is controlled mainly by the spontaneous fission and  $\alpha$ -decay processes [1–4, 6–12]. An important factor in the decay process of superheavy nuclei is the shell effect. It supplies the extra binding energy and increases the barrier height of fission [13–18]. The situation in the case of spontaneous fission is very complex as compared to the  $\alpha$ -decay process along the stability line of the superheavy region. Further, there is also the possible  $\beta^-$ -decay mode for the superheavy nuclei that proceeds via the weak interaction. This process is slower and less favored as compared to spontaneous fission and  $\alpha$ -decay in the valley of stability.

The most stable superheavy nuclei are predicted to be located along the neutron rich region of the  $\beta$ -stability line. It is not possible to reach those directly by the above mentioned fusion reactions with stable ion beams. In fact, the predicted magic proton number for the superheavy region are quite different within various theoretical approaches. For example, the magic proton number  $Z = 114$  was predicted in the earliest macro-microscopic calculations [19, 20], and later confirmed by Refs. [14, 21]. Fully microscopic approaches predict the proton shell closure at  $Z = 120$  [22–24], and/or  $Z = 126$  [25] using selected nucleon-nucleon interactions in mean field models. The neutron magic number  $N = 184$  is almost firmly predicted by different theoretical models [21, 24]. For fur-

ther experimental study of the superheavy nuclei, especially near the neutron rich side of the nuclear chart, basic ideas of the internal structure and reaction mechanism of those nuclei from advanced theoretical approaches are required. In other words, in order to produce superheavy nuclei in the laboratory, one needs to know the internal configuration and the radioactive decay properties theoretically. Hence, the knowledge of the modes of decay and half-lives of a nucleus over a very wide range of neutron-proton asymmetry within advanced theories are essential for their synthesis process and further progress in experiments.

In this regard, we investigate different possible modes of radioactive decay for the neutron rich superheavy nuclei. We have used the relativistic mean field (RMF) formalism [26, 27] with the recently developed NL3\* interaction parameter  $s$ [28] for the present analysis. The model have been successfully applied in the description of nuclear structure phenomena both in  $\beta$ -stable and  $\beta$ -unstable regions throughout the nuclear landscape including superheavy nuclei [26–38]. The constant strength scheme is adopted to take into account pairing correlations [30, 39] and evaluate the pairing gaps for neutrons and protons using the BCS equations [41]. The aim of the present study is to determine the properties of the modes of decay of neutron rich superheavy nuclei, which may help us to answer some important open questions: (1) how far may we still move in synthesis of superheavy elements by the fusion reactions, (2) where the island of stability is centered, (3) what are the properties of the most stable superheavy nuclei, and (4) how can one reach to this region. Further, the decay properties also play a crucial role in the study of the  $r$ -process of nucleosynthesis as well as the formation of heavy and superheavy nuclei in nature [42, 43]. Here we have considered the isotopic chains  $Z = 118$  and  $120$  with  $160 \leq N \leq 204$ , predicted to be the next magic valley [23, 24, 44] after  $^{208}\text{Pb}$ . The basic idea is that the decay process is highly influenced by the internal configuration of the nucleus. In other words, the internal arrangement of nucleons determines the stability and modes of decay of the nucleus.

We have thus tried to explain the modes of decay of superheavy nuclei, by means of their internal structure

\* Email: bhuyan@ita.br

† Email: brettvc@gmail.com

TABLE I. The RMF (NL3\*) result for binding energy, root-mean-square charge radius  $r_{ch}$ , the quadrupole deformation parameter  $\beta_2$ , the energy difference between the ground and first intrinsic excited state ( $\Delta E$ ) and the relative neutron-proton asymmetry at the surface to the center  $R_\eta$  for  $^{278-322}_{118}$ .

Nucleus	BE	$\beta_2$	$r_{ch}$	$\Delta E$	$R_\eta$
$^{278}_{118}$	1966.5	0.258	6.271	0.258	2.51
$^{280}_{118}$	1983.4	0.553	6.495	0.553	2.54
$^{282}_{118}$	2000.1	0.553	6.507	0.553	2.58
$^{284}_{118}$	2016.1	0.554	6.520	0.554	2.61
$^{286}_{118}$	2031.7	0.551	6.529	0.551	2.64
$^{288}_{118}$	2046.8	0.543	6.535	0.543	2.69
$^{290}_{118}$	2061.7	0.533	6.538	0.533	2.71
$^{292}_{118}$	2076.3	0.528	6.546	0.528	3.04
$^{294}_{118}$	2090.2	0.535	6.563	0.535	3.16
$^{296}_{118}$	2103.5	0.544	6.582	0.544	3.20
$^{298}_{118}$	2116.2	0.554	6.602	0.554	3.33
$^{300}_{118}$	2128.3	0.564	6.624	0.564	3.47
$^{302}_{118}$	2140.0	0.580	6.651	0.580	3.61
$^{304}_{118}$	2151.2	0.582	6.667	0.582	3.96
$^{306}_{118}$	2161.6	0.590	6.688	0.590	4.11
$^{308}_{118}$	2171.6	0.609	6.721	0.609	4.26
$^{310}_{118}$	2181.3	0.622	6.747	0.622	4.41
$^{312}_{118}$	2192.8	0.753	6.893	0.753	4.57
$^{314}_{118}$	2202.6	0.766	6.923	0.766	4.71
$^{316}_{118}$	2212.1	0.776	6.950	0.776	4.87
$^{318}_{118}$	2216.9	0.571	6.749	0.571	4.94
$^{320}_{118}$	2225.6	0.525	6.720	0.525	5.06
$^{322}_{118}$	2233.7	0.534	6.739	0.534	5.13

and sub-structure. To know the proper internal configuration, it is important to know the ground and first intrinsic excited state properties of the nucleus. The bulk properties such as binding energy (BE), root mean square charge radii  $r_{ch}$ , matter radii, and the energy difference between the ground state and the intrinsic first excited state  $\delta E$  are calculated using the NL3\* force parameter. The results for the isotopic chains of  $Z = 118$  and  $Z = 120$  are listed in Table. I and II, respectively. The quantity ( $R_\eta$ ) in the last column of both the tables will be discussed in subsequent sections. The ground state solutions for the isotopic chains of  $Z = 118$  and 120 have a deformed prolate configuration while the first excited states are found to be of spherical shape. An analysis of the internal structure of the nucleus is possible from the three dimensional (3D) contour plot of the deformed density. Here, we show the total density distribution, which is the sum of the proton  $\rho_p$  and neutron  $\rho_n$  density of the nucleus for the ground state solution. The total density of the nucleus extends from the center to a distance of about  $7 fm$ , as seen in Figs. 1, 2 and 3.

Due to their symmetry, the densities need only be obtained for the positive quadrant of the plane parallel to the  $z$ -axis (the symmetry axis), and are evaluated in the  $r_\perp z$ -plane, where  $x = r_\perp \cos\varphi$  and  $y = r_\perp \sin\varphi$  (cylindrical coordinates). The contour plots of the total density for the ground state of  $Z=118$  and 120 for  $N = 172, 182$

TABLE II. The RMF (NL3\*) result for binding energy, root-mean-square charge radius  $r_{ch}$ , the quadrupole deformation parameter  $\beta_2$ , the energy difference between the ground and first intrinsic excited state ( $\Delta E$ ) and the relative neutron-proton asymmetry at the surface to the center  $R_\eta$  for  $^{280-324}_{120}$ .

Nucleus	BE	$\beta_2$	$r_{ch}$	$\Delta E$	$R_\eta$
$^{280}_{120}$	1962.54	0.258	6.300	0.058	2.51
$^{282}_{120}$	1980.67	0.248	6.307	0.201	2.54
$^{284}_{120}$	1997.28	0.233	6.309	0.926	2.57
$^{286}_{120}$	2013.78	0.567	6.306	0.340	2.63
$^{288}_{120}$	2029.97	0.562	6.309	0.929	2.68
$^{290}_{120}$	2045.56	0.556	6.313	0.301	2.71
$^{292}_{120}$	2060.87	0.547	6.285	0.729	2.75
$^{294}_{120}$	2075.85	0.541	6.385	0.916	2.81
$^{296}_{120}$	2090.29	0.545	6.400	2.394	2.87
$^{298}_{120}$	2104.30	0.554	6.305	0.058	2.91
$^{300}_{120}$	2117.63	0.564	6.311	3.291	3.99
$^{302}_{120}$	2130.28	0.586	6.318	3.691	3.11
$^{304}_{120}$	2142.57	0.591	6.326	4.462	3.21
$^{306}_{120}$	2154.10	0.596	6.340	4.744	3.38
$^{308}_{120}$	2164.84	0.600	6.747	4.439	3.43
$^{310}_{120}$	2175.19	0.614	6.831	4.727	3.61
$^{312}_{120}$	2186.32	0.726	6.858	5.396	3.79
$^{314}_{120}$	2196.88	0.726	6.880	5.837	3.94
$^{316}_{120}$	2206.90	0.729	6.642	5.797	4.07
$^{318}_{120}$	2216.86	0.742	6.643	5.743	4.16
$^{320}_{120}$	2221.24	-0.436	6.634	0.707	4.27
$^{322}_{120}$	2230.56	-0.445	6.618	0.765	4.41
$^{324}_{120}$	2239.09	-0.448	6.606	0.544	4.63

and 204 are shown in the lower panel of Figs. 1, 2 and 3, respectively. The color code along with the density ranges are given on the right side of the contour plots. From the color code, we can determine the range of the density values for a specific region of the nucleus (i.e. the cluster structures). For example, the color code with *deep red* corresponds to maximum density value ( $\rho \sim 0.18 fm^{-3}$ ) and the *deep blue* to the minimum density ( $\rho \sim 0.001 fm^{-3}$ ). A careful inspection of the contour plots of the ground state density distributions shows a broken *ring*-like structure at the surface of the isotopes along the valley of stability. The distorted *ring*-like structure in the case of proton rich isotopes for  $N = 172$  ( $^{290}_{118}$  and  $^{292}_{120}$ ) (Fig. 1) disappears as one moves towards the neutron rich isotopes (Fig. 2). The asymmetry of the density in the *ring*-like region is higher than that of the central region of a nucleus. It shows a clear signature of a neutron skin structure for the neutron rich isotopes of  $Z = 118$  and 120. This special attribute in the surface region of the nucleus also could play crucial role in the mode of decay of these nuclei.

The asymmetry parameter  $\eta$  can be estimated from the mean field density distributions and is defined as,

$$\eta = \frac{(\rho_n - \rho_p)}{(\rho_n + \rho_p)}. \quad (1)$$

Here,  $\rho_n$  and  $\rho_p$  are the density distribution of the proton

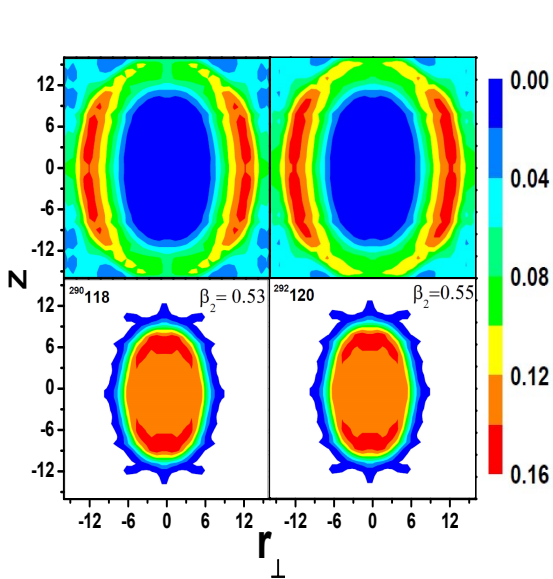


FIG. 1. (Color online) The total ground state density and the neutron-proton asymmetry parameter  $\eta$  distribution for the density of  $^{290}_{118}$  and  $^{292}_{120}$  from the relativistic mean field (RMF) with NL3\* force are displayed in the lower and upper panels, respectively.

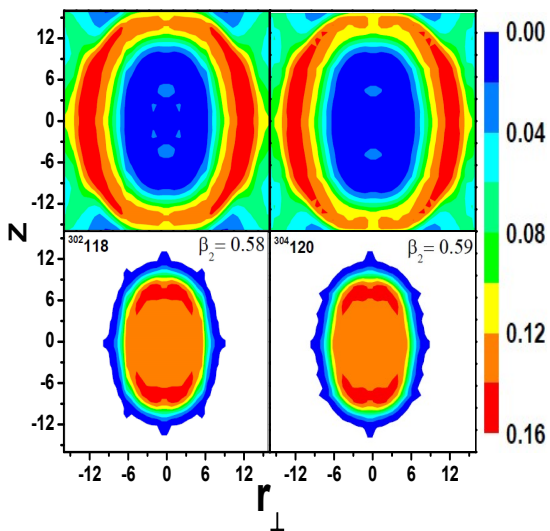


FIG. 2. (Color online) The total ground state density and the neutron-proton asymmetry parameter  $\eta$  distribution for the density of  $^{302}_{118}$  and  $^{304}_{120}$  from the relativistic mean field (RMF) with NL3\* force are displayed in the lower and upper panels, respectively.

and neutron, respectively. The role of this parameter is essential for estimation of the predominant constituents (neutron or/and proton) for a specific region. In other words, the contour plots of the asymmetry parameter  $\eta$  using Eq. (1) shows the neutron-proton asymmetry distributions of the nucleus. The contour plots of  $\eta$  for selected isotopes such as  $^{290,302,322}_{118}$  and  $^{292,304,324}_{120}$

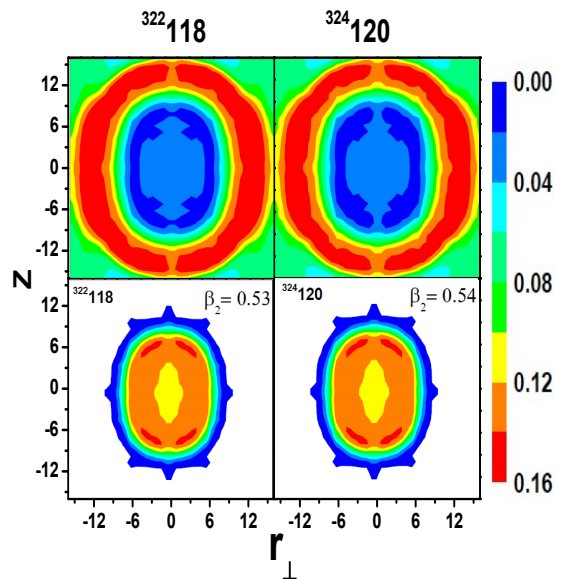


FIG. 3. (Color online) The total ground state density and the neutron-proton asymmetry parameter  $\eta$  distribution for the density of  $^{322}_{118}$  and  $^{324}_{120}$  from the relativistic mean field (RMF) with NL3\* force are displayed in the lower and upper panels, respectively.

are shown in the upper panel of the Figs. 1, 2 and 3. The values of  $\eta$  along with color codes are given to the right of the figure. From the figure, we find the distribution of the asymmetry parameter is uniform in the center of the nuclei but increases to a very high value (i.e. almost four times the central value) and forms a *ring*-like structure at the surface. Quantitatively, the central region (i.e.  $\sim 0 - 5fm$ ), has a value of  $\eta \sim 0.2$ , which changes to  $\sim 0.8$  at the surface region (i.e.  $\sim 5 - 8fm$ ). Note that that the value of  $\eta$  is divided by 5 to use the color code in the right side of the figures. Here, we also find a *ring*-like structure for all the isotopes (Fig. 3), but the situation is just reverse the of the ground state density (see Fig. 2). The *ring*-like structures is also shifted toward the surface with increase of the neutron number. The concentration of neutrons in the surface region suggests a strong possibility for  $\beta^-$ -decay. Calculations in triaxially deformed coordinate space may resolve more issues and will throw more light on this possibility.

We have estimated the relative neutron-proton asymmetry at the surface to that at the center of the nucleus  $R_{\eta} = \eta_s/\eta_c$  (i.e. the ratio of the average asymmetries of the surface  $\eta_s$  to the center  $\eta_c$ ) for the isotopic chains of  $Z = 118$  and  $Z = 120$ . The estimated values of relative neutron-proton asymmetry parameter  $R_{\eta}$  are listed in the last column of Tables I and II for the  $Z = 118$  and  $120$  isotopes, respectively. We find that the magnitude of  $R_{\eta}$  increases with neutron number in each isotopic chain. The values of the  $R_{\eta}$  is  $\sim 2.5$  for  $^{290}_{118}$  (i.e.  $N=172$ ) and increase gradually with the neutron number, reaching a value of 5.0 for  $^{322}_{118}$ . We see a similar tendency for the isotopic chain of  $Z = 120$  (i.e. see Table II). The

excess neutrons clearly accumulate in the surface region instead of the center of the nucleus. This effect is also manifested in the progressive appearance of a neutron *ring*-like structure with high neutron density. Due to the extreme neutron richness at the surface,  $\beta^-$ -decay could become a predominant mode of decay of neutron rich superheavy nuclei instead of  $\alpha$ -decay. It might also be an alternative to the fission process of highly neutron rich nuclei [13, 45], where the process is inhibited due to extreme neutron richness in the neck region.

In summary, we have analyzed the bulk properties such as the binding energy, charge radius  $r_{ch}$ , and the binding energy difference of ground and intrinsic first excited states  $\Delta_E$  for the isotopic chains of  $Z = 118$  and  $120$ . The RMF model, which has gained the confidence of the nuclear community in the study of exotic nuclei includ-

ing superheavy nuclei has been adopted for the present study. We found deformed prolate ground state structure for these nuclei and a spherical first excited state. The ground state density along with the asymmetry parameter  $\eta$  are also calculated. The widely varying relative neutron-proton asymmetry at the surface to that of the center of a nucleus  $R_\eta$  suggests a possible  $\beta^-$ -decay mode. To our knowledge, this is one of the first such interesting and different phenomenon to appear in the superheavy region.

This work is supported in part by FAPESP Project Nos. (2014/26195-5 & 2017/05660-0), INCT-FNA Project No. 464898/2014-52014/26195-5, and CNPq-Brasil. The authors are also thankful to S. K. Patra, Institute of Physics, for discussions and also for support throughout the work.

- 
- [1] S. Hofmann and G. Münzenberg, *Rev. Mod. Phys.* **72**, 733 (2000).
- [2] S. Hofmann *et al.*, *Z. Phys. A* **350**, 277 (1995).
- [3] S. Hofmann *et al.*, *Z. Phys. A* **354**, 229 (1996).
- [4] S. Hofmann *et al.*, *Rep. Prog. Phys.* **61**, 639 (1998);
- [5] S. Hofmann *et al.*, *Acta Phys. Pol. B* **30**, 621 (1999).
- [6] Yu. Ts. Oganessian, *Phys. Rev. Lett.* **83**, 3154 (1998).
- [7] Yu. Ts. Oganessian *et al.*, *Nucl. Phys. A* **685**, 17c (2001).
- [8] Yu. Ts. Oganessian *et al.*, *Phys. Rev. C* **69**, 021601(R) (2004).
- [9] Yu. Oganessian, *J. Phys. G: Nucl. Part. Phys.* **34**, R165 (2007).
- [10] Yu. Ts. Oganessian *et al.*, *Phys. Rev. Lett.* **104**, 142502 (2010).
- [11] Yu. Ts. Oganessian *et al.*, *Phys. Rev. C* **83**, 954315 (2011).
- [12] R. Eichler *et al.*, *Nucl. Phys. A* **787**, 373c (2007).
- [13] L. Satpathy and S.K. Patra, *J. Phys. G* **30**, 771 (2004).
- [14] Z. Patyk and A. Sobczewski, *Nucl. Phys. A* **533**, 132 (1991).
- [15] D. N. Poenaru, I. H. Plonski, W. Greiner, *Phys. Rev. C* **74**, 014312 (2006).
- [16] C. Samanta, D. N. Basu, P. R. Chowdhury, *J. Phys. Soc. Japan* **76**, 124201 (2007).
- [17] D. S. Delin, R. J. Liotta, R. Wyss, *Phys. Rev. C* **76**, 044301 (2007).
- [18] H. F. Zhang, G. Royer, *Phys. Rev. C* **76**, 047304 (2007).
- [19] H. Meldner, *Ph.D. thesis*, University Frankfurt am Main (1966).
- [20] S. G. Nilsson, C. F. Tsang, A. Sobczewski, Z. Szymanski, S. Wycech, C. Gustafson, I.-L. Lamm, P. Möller, and B. Nilsson, *Nucl. Phys.*, A **131**, 1 (1969).
- [21] P. Möller and J. R. Nix, *Nucl. Phys.*, A **549**, 84 (1992).
- [22] M. Beiner, H. Flocard, M. Vèneroni, and P. Quentin, *Phys. Scr.*, **10A**, 84 (1974).
- [23] S. Ahmad, M. Bhuyan, and S. K. Patra, *Int. J. Mod. Phys. E* **21**, 1250092 (2012).
- [24] M. Bhuyan, and S. K. Patra, *Mod. Phys. Lett. A* **27**, 1250173 (2012).
- [25] S. Œwiok, J. Dobaczewski, P.H. Heenen, P. Magierski, W. Nazarewicz, *Nucl. Phys.*, A **611**, 211 (1996).
- [26] J. Boguta and A. R. Bodmer, *Nucl. Phys. A* **292**, 413 (1977).
- [27] B. D. Serot and J. D. Walecka, in *Advances in Nuclear Physics*, edited by J. W. Negele and Erich Vogt *Plenum Press, New York*, Vol. **16**, p. 1 (1986).
- [28] G. A. Lalazissis, S. Karatzikos, R. Fossion, D. Pena Arteaga, A. V. Afanasjev, and P. Ring, *Phys. Lett. B* **671**, 36 (2009).
- [29] G. A. Lalazissis, S. Raman and P. Ring, *Atm. Data. Nucl. Data. Table.* **71**, 1 (1999).
- [30] S. K. Patra, M. Bhuyan, M. S. Mehta and Raj K. Gupta, *Phys. Rev. C* **80**, 034312 (2009).
- [31] M. Bhuyan, S. K. Patra, and Raj K. Gupta, *Phys. Rev. C* **84**, 014317 (2011).
- [32] P. Ring, *Prog. Part. Nucl. Phys.* **37**, 193 (1996).
- [33] D. Vretenar, A. V. Afanasjev, G. A. Lalazissis, and P. Ring, *Phys. Rep.* **409**, 101 (2005).
- [34] J. Meng, H. Toki, S. G. Zhou, S. Q. Zhang, W. H. Long, and L. S. Geng, *Prog. Part. Nucl. Phys.* **57**, 470 (2006).
- [35] T. Niksić, D. Vretenar, and P. Ring, *Prog. Part. Nucl. Phys.* **66**, 519 (2011).
- [36] Xian-Feng Zhao, and Huan-Yu Jia, *Phys. Rev. C* **85**, 065806 (2012).
- [37] M. Bhuyan, S. K. Patra, and Raj K. Gupta, *J. Phys. G: Nucl. Part. Phys.*, **42**, 015105 (2015).
- [38] M. Bhuyan, *Phys. Rev. C* **92**, 034323 (2015).
- [39] M. Del Estal, M. Centelles, X. Viñas and S. K. Patra, *Phys. Rev. C* **63**, 044321(2001);
- [40] M. Del Estal, M. Centelles, X. Viñas and S.K. Patra, *Phys. Rev. C* **63**, 024314 (2001).
- [41] M. A. Preston and R. K. Bhaduri, *Structure of the nucleus*, (Addition-Wesley Publishing Co.), p-144 (1975).
- [42] I. V. Panov, I. Yu. Korneev, and F.-K. Thielemann, *Phys. Atm. Nucl.*, **72**, 1026 (2009).
- [43] S. Goriely, G. M. Pinedo, *Nucl. Phys. A* **944**, 158 (2015).
- [44] S. K. Patra, W. Greiner and R. K. Gupta, *J. Phys. G: Nucl. Part. Phys.* **26**, L65 (2000).
- [45] S. K. Patra, R. K. Choudhury, and L. Satpathy, *J. Phys. G: Nucl. Part. Phys.* **37**, 085103 (2010).